2023 6th International Conference on Pattern Recognition and Image Analysis (IPRIA)
Faculty of Engineering, College of Farabi, University of Tehran, Iran, 14-16 February 2023

Contextual Information Classification of Remotely Sensed Images

Alirza Dori
Image processing and Information Analysis Lab, Faculty of Electrical and Computer Engineering
TarbiatModares University
Tehran, Iran
a.dori@modares.ac.ir

Hassan Ghassemian
Image processing and Information Analysis Lab, Faculty of Electrical and Computer Engineering
TarbiatModares University
Tehran, Iran
ghassemi@modares.ac.ir

Maryam Imani
Image processing and Information Analysis Lab, Faculty of Electrical and Computer Engineering
TarbiatModares University
Tehran, Iran
maryam.imani@modares.ac.ir

***Abstract*— This work proposes a multidisciplinary contextual information extraction and decision fusion approach for increasing the classification accuracy. It improves the image classification with integrating the results of various classifiers. The proposed method is implemented in three-steps: 1) contextual feature extraction using four different feature extractors methods: a) Gray Level Cooccurrence Matrix ,b) Gabor filters, c) Laplacian Gaussian filters and d) Gaussian Derivatives Functions; 2) classification of contextual features using four different classification rules (ML, Tree, KNN and SVM) by using only 2% of data for training the classifiers; and 3) finally, decision fusion using six decision fusion rules. The experimental results on real remotely sensed images have been presented.**

Keywords*— *contextual information, feature extraction, classification, decision fusion, remote sensing.

I. Introduction

Development of remote sensing satellite technology has provided a great ability to produce multispectral images. These images are taken at different wavelengths of the electromagnetic spectrum with different spectral, temporal, spatial and radiometric resolutions. Due to practical limitations in construction of sensors, it is not possible to obtain images that have both spectral and spatial accuracy [1,2]. The image integration process can be used to overcome this problem. In this process, spatial information is extracted from images with high spatial resolution and spectral information is extracted from images with high spectral resolution. Then, by integrating them, an image with both high spatial and spectral resolution is generated. These fused images contain various features that differ in spectral, spatial, temporal, and radiometric resolution. Thus, they provide a complete view of the observed objects. It leads to an improved classification accuracy.

The main stage of image classification is selecting training samples, preprocessing, feature extraction, selecting the appropriate classification, post-processing, and validation [3]. One of the effective factors in increasing the classification accuracy is the given features. Selecting appropriate features is an important step for the successful implementation of image classification. Using too many features in a classification method may reduce the classification accuracy. (Hughes phenomenon). It is important to only select variables that are useful for separating classes. The commonly used features in classification of remote sensing images are categorized into two main groups: spectral features and spatial features. The spectral feature vector of a pixel is a vector whose elements are the reflected energy from a point in the scene corresponding to different spectral bands. Also, spatial features can be divided into two main categories: texture and shape features. Texture properties act as a measure of roughness, smoothness and image details.

In recent years, various methods have proposed for improvement of images classification. For example, the following methods can be referred: integration of fractal and spectral features [4], using convolutional neural network (CNN) methods and naïve Gabor Nets [5], morphology-based structure-preserving projection (MSPP) [6], and the Pixon-based image segmentation method [7]. As we expected, by using the spatial features of image such as shape, texture and geometrical structures, the land cover discrimination will be improved.

Researchers have proposed different methods to model the contextual information from images such as Markov random fields [8], 3-D Gabor feature extraction [9], edge-preserving filtering [10], sparse representation model [11], hybrid-graph learning method [12]-[13], morphological feature-based method [14]-[15] and deep learning-based method [16].

In this work, in order to increase the classification accuracy of contextual information, we used four different methods for feature extraction: Gray Level co-occurrence matrix [17], Gabor filters [17], Laplacian Gaussian filters [18] and Gaussian Derivative Functions [19]. Then, we classify each of the obtained features with four different classification rules (ML, Tree, KNN and SVM). Finally, we did decision fusion using majority voting (MV), Weighted majority voting (WMV), maximum, sum, product and Dempster-Shafer Theory (DST). DST method is used in many studies recently [20]. The two methods WMV and DST are very accuracy, but the DST method is much more complicated than WMV.

II. Proposed Decision Fusion Methods

A) Feature Extraction and Classification

In general, it can be said that the information of an image includes color, texture, shape or edge. The color information of the image can be obtained from the multispectral image and its shape and texture can be obtained from the panchromatic image.

979-8-3503-1455-7/23/$31.00 ©2023 IEEE

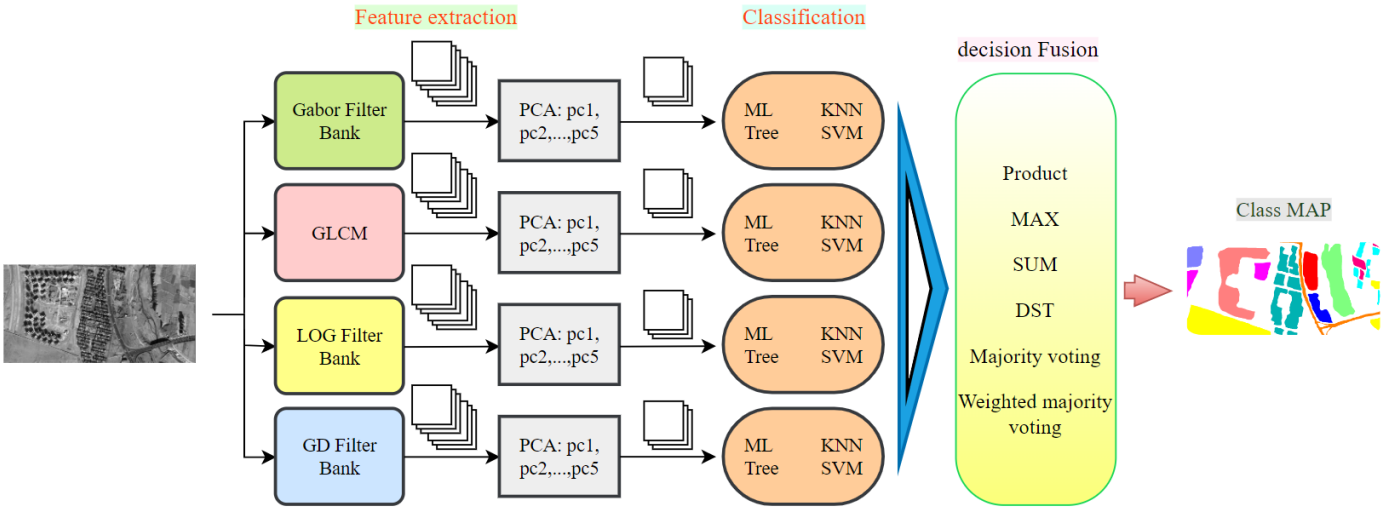

Fig.1 Framework of contextual information classification.

In this paper, we performed feature extraction using gray level co-occurrence matrix (GLCM), Gabor filter, Laplacian of Gaussian filter (LOG) and Gaussian partial derivatives (GD).

GLCM provides a high level of discrimination power to texture patterns by parametrically describing the spatial arrangement of pixels. GLCM is a complex matrix form constructed in a local window, consisting of probability density values of all pixel gray surfaces. Gabor filters are other useful tools for achieving joint space and frequency resolutions. A Gabor filter bank is composed from Gabor filters with various directions and scales. So, a Gabor filter bank can achieve the localization characterizations in frequency and spatial domains. A filter bank is formed by using Gabor filter at different rotation angles and scales. Another method for deriving spatial properties is to use the partial derivative of Gaussian and Laplacian of Gaussian. This method is based on derivation. Since the edge is the place where the changes occur, measuring the changes using the derivative operation can identify the edges. However, because image derivation amplifies the noise, the derivation is performed on a Gaussian filtered image, and the resulting filter is used to extract spatial features. In this approach, we formed a filter bank for LOG filter and GD like Gabor filter.

$$\text{GD filter bank} \sim \left\{ \mathbf{G}^{(n+m)}(\boldsymbol{x},\boldsymbol{y}) = \frac{\partial^n}{\partial \boldsymbol{x}^n} \cdot \frac{\partial^m}{\partial \boldsymbol{y}^m} \mathbf{G}(\boldsymbol{x},\boldsymbol{y}) \quad \boldsymbol{n},\boldsymbol{m} \in \boldsymbol{N} \cup \{\mathbf{0}\} \right\} \quad (1)$$

Table I. Parameters of contextual feature extraction methods

Feature type	Parameter	number of Features
Gabor Filter	$Ns = 6$, $Nd = 4$, $Sx = 1.5$, $Sy = 2$, winLen ∈ { 2, 4, 8, 16, 32, 64 }	24
LOG Filter	$Ns = 6$, $Nd = 4$, $Sx = 1$, $Sy = 1$, winLen ∈ {17, 33, 57, 97, 199, 397}	24
GLCM	θ = {0} $d = 1$ winLen = 33	16
GD Filter	winLen = 35 N=6	26

Filter bank of LOG is similar to Gabor filter bank built by rotating the main wavelet in different directions with different frequencies. The LOG filter is inspired by the human visual attention system [21]. The GD filter bank is due to Gaussian filter derivative order where $N = n + m$ is order of derivative operation.

Then, we apply the principal component analysis (PCA) to hyperspectral data and obtain the first five principal component (PC1, PC2…PC5) from it. After that, we apply different classification methods to it. The proposed block diagram is shown in Fig.1. The proposed method uses GLCM, Gabor filter, Laplacian of Gaussian filter (LOG) and Gaussian partial derivatives (GD) approach for feature extraction, and ML, Tree, KNN (k = 1) and SVM classifiers.

B) Decision Fusion Method

As mentioned, in this step, after feature extraction and classification of image with various mentioned methods, we combine the output of the classifiers to improve the classification accuracy.

For this purpose, we assign a degree of belonging to given classes to each pixel of the image. This degree of belonging is calculated from the output results for each class. Consider $conf_i$ as the confusion matrix obtained from the local classification results.

In addition, we suppose that N_{C_i} is the total number of pixels related to class C_i and n_{ij} is the number of pixels related to class C_i but assigned to class C_j [22-24]:

$$conf_i \triangleq [n_{ij}] = \begin{bmatrix} n_{11} & n_{12} & \cdots & n_{1m} \\ n_{21} & n_{22} & \cdots & n_{2m} \\ \vdots & \vdots & \cdots & \vdots \\ n_{m1} & n_{m2} & \cdots & n_{mm} \end{bmatrix} \quad (2)$$

$$N_{C_i} = \sum_j n_{ij} \quad , N^*_{C_j} = \sum_i n_{ij} \quad (3)$$

where $N^*_{C_j}$ is the total number of assigned pixels to the class C_j. Now, we define the $\overrightarrow{va}_{C_i}$ and $\overrightarrow{ac}_{C_i}$ as the accuracy and validity vector of i^{th}classifier and cth class results:

$$\overrightarrow{va}_{C_i} = [va_{1i}\ va_{2\mathrm{i}} \quad \cdots \quad va_{\mathrm{ni}}]^T \tag{4}$$

$$\overrightarrow{ac}_{C_i} = [ac_{i1}\ \ ac_{\mathrm{i2}} \quad \cdots \quad ac_{\mathrm{in}}]^T \tag{5}$$

$$va_{ij} = \frac{n_{ij}}{\sum_i n_{ij}} = \frac{n_{ij}}{N_{C_j}^{\ *}} \tag{6}$$

$$ac_{\mathrm{ij}} = \frac{n_{ij}}{\sum_j n_{ij}} = \frac{n_{ij}}{N_{C_i}} \tag{7}$$

In the proposed method, to obtain the degree of belonging, we use the accuracy vectors ($\overrightarrow{ac}_{C_i}$) and validity vectors ($\overrightarrow{va}_{C_i}$) and then obtain the degree of belongness vector (class membership number) by combining these two vectors as follows:

$$\boldsymbol{m}_{C_{ij}}=\mathrm{f}\,(ac_{\mathrm{ij}}(\mathrm{k}),\, va_{ij}(\mathrm{k})) \tag{8}$$

$$\mathrm{f}\,(ac_{\mathrm{ij}}(\mathrm{k}),\, va_{ij}(\mathrm{k})) = ac_{\mathrm{ij}}(\mathrm{k}).\, va_{ij}(\mathrm{k})$$

$$\mathrm{f}\,(ac_{\mathrm{ij}}(\mathrm{k}),\, va_{ij}(\mathrm{k})) = ac_{\mathrm{ij}}(\mathrm{k}) + va_{ij}(\mathrm{k})\text{-}ac_{\mathrm{ij}}(\mathrm{k}).\, va_{ij}(\mathrm{k})$$

Then, we use methods such as max, sum, product and the Dempster-Shafer theory for decision fusion. The selected class as the result of fusion is a class which includes the maximum value of $\boldsymbol{m}_{C_{\mathrm{i}}}^{1\oplus 2\ldots\oplus N}$ (fused vector function). In which, $\oplus$ is symbol of the fusion classifiers. In other words, we have:

$$\mathrm{X}\in C_k \quad \text{if} \quad ; \quad \boldsymbol{m}_{C_k}^{1\oplus 2\ldots\oplus N} = max_{C_{\mathrm{i}}}\{\boldsymbol{m}_{C_{\mathrm{i}}}^{1\oplus 2\ldots\oplus N}\} \tag{9}$$

Table II. Different decision fusion rules

Name of method	**Formula**
Max	$\boldsymbol{m}_{C_{\mathrm{i}}}^{1\oplus 2\ldots\oplus N}=\max(\boldsymbol{m}_{C_{\mathrm{i}}}^{1}, \boldsymbol{m}_{C_{\mathrm{i}}}^{2} \ldots., \boldsymbol{m}_{C_{\mathrm{i}}}^{N})$
sum	$\boldsymbol{m}_{C_{\mathrm{i}}}^{1\oplus 2\ldots\oplus N}= \boldsymbol{m}_{C_{\mathrm{i}}}^{1} + \boldsymbol{m}_{C_{\mathrm{i}}}^{2} + \cdots + \boldsymbol{m}_{C_{\mathrm{i}}}^{N}$
Product	$\boldsymbol{m}_{C_{\mathrm{i}}}^{1\oplus 2\ldots\oplus N}= \boldsymbol{m}_{C_{\mathrm{i}}}^{1} \times \boldsymbol{m}_{C_{\mathrm{i}}}^{2} \times \ldots \times \boldsymbol{m}_{C_{\mathrm{i}}}^{N}$
DST	$\mathrm{m}_{12}(\mathrm{A}) = \mathrm{m}_1(\mathrm{A_i}) \oplus \mathrm{m}_2(\mathrm{A_j}) = \frac{\sum_{\mathrm{A_i}\cap\mathrm{A_j}=\mathrm{A}} \mathrm{m}_1(\mathrm{A_i})\times\mathrm{m}_2(\mathrm{A_j})}{1-\mathrm{K}}$; $\mathrm{H}\neq\emptyset$ $\mathrm{K}=\sum_{\mathrm{A_i}\cap\mathrm{A_j}=\emptyset} \mathrm{m}_1(\mathrm{A_i}) \times \mathrm{m}_2(\mathrm{A_j})$

Also we use MV method and Weighted MV (WMV) for fusion result. For the WMV method, depending on the size of accuracy and validity of each class and classifier, a weight is assigned to each result, which has an integer value between 0 and 4. Then we calculate number of repeat of weighted Class and select maximum repeat as the chosen class. Despite the simplicity of the WMV method, the results of this method are comparable to complex methods such as DST.

III. Experiments

Experiments were done on three data sets. The first dataset is a panchromatic image consisting of 908 × 1892 pixels from a small town near Tehran which includes 12 different classes. The second dataset is 8 pieces from different areas of Tehran which are cut and placed next to each other. The third dataset shows a panchromatic and a multispectral image of a specific area, which include three spectral bands and the information of these bands is available as a 512 × 512 matrix. Implementation was done on the three introduced datasets. The classification map results for these datasets are shown in Figs. 3,5,6. (dataset are available in the google drive link: https://drive.google.com/drive/folders/1OYYEqvqOuvD7GjOlDngwDZlk0yJrUXuT?usp=sharing).

As expected, classifying individual classification of spatial information does not lead to sufficient accuracy. So, to achieve results with more accurate, these categories are combined by decision fusion methods. The classification results are quantitatively evaluated by measuring the overall accuracy (OA), Average accuracy (AA), kappa coefficient (κ) and average validity (AV). Tables III represent the classification results.

IV. Conclusion

In this paper, we use decision fusion method to improve image classification. First, we got contextual information and then classify it with several classifiers. Finally, we fused the classification results. The experimental results showed an improvement of the classification accuracy. In this article, we described one of the most important methods of decision fusion, which is called the Dempster-Shafer method. We implemented it to improve the classification performance. We used the accuracy and validity vectors for belonging degree of each pixel to the given classes. We showed that by using methods such as addition and multiplication, the classification results could be improved. Using the neural network [25,26] to achieve the desired results requires lots of training data. But by combining feature extraction and using machine learning, we were able to achieve accurate results.

By comparing the results of data classification for different data sets, it is clear that the Sum and Product and WMV methods lead to higher accuracy compared to other methods. Given that we used square windows with different sizes to extract the content features, the results of data set give less accurate results in border areas especially in first data set. The second dataset shows images of eight districts of Tehran that are placed next to each other in pieces. The problem with these data is that the data is artificial, and this result may not be true for real data. Therefore, to investigate this issue, the results have been tested on the third dataset. The third set shows a real data that the reference map by Photoshop software has been made. The construction of the reference map is such that we identified the similar pixels were identified by eye comparison with a label and thus formed 7 different classes for this database. In this database, WMV methods, Product and DST lead to high accuracy.

Fig.2. Panchromatic Images of Dataset 1

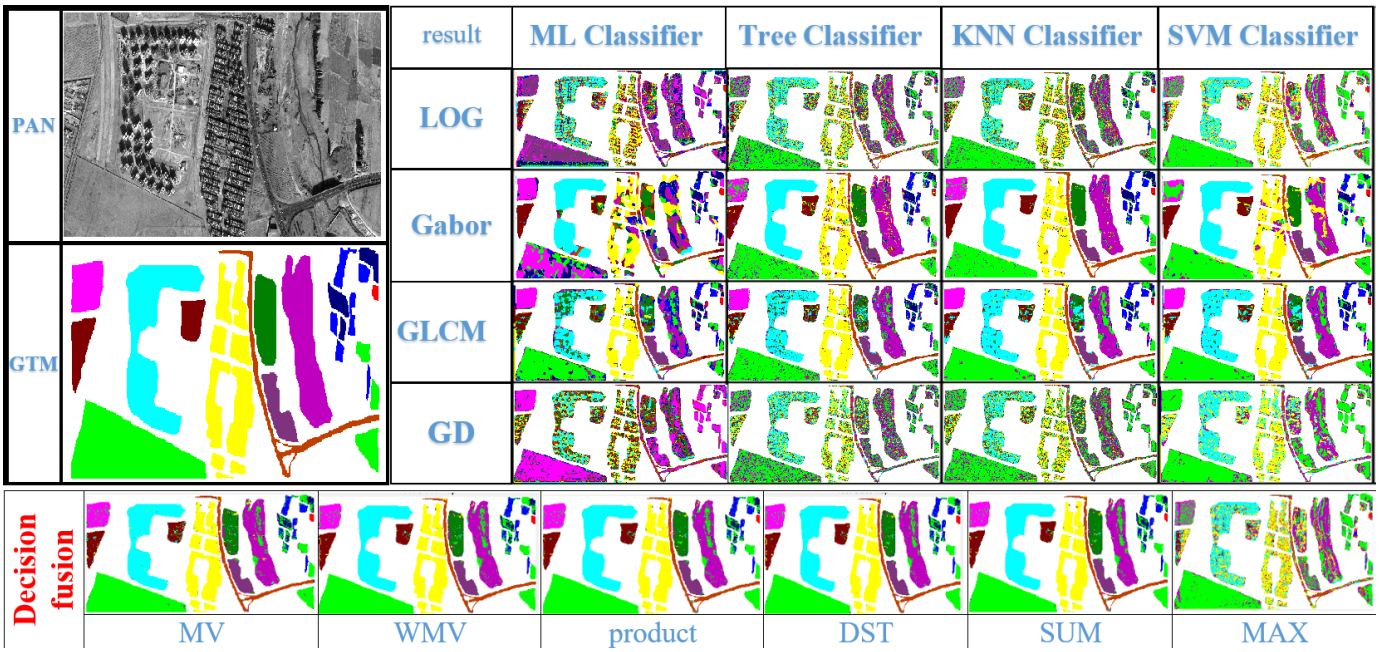

Fig. 3 The reference map and classification maps of dataset 1

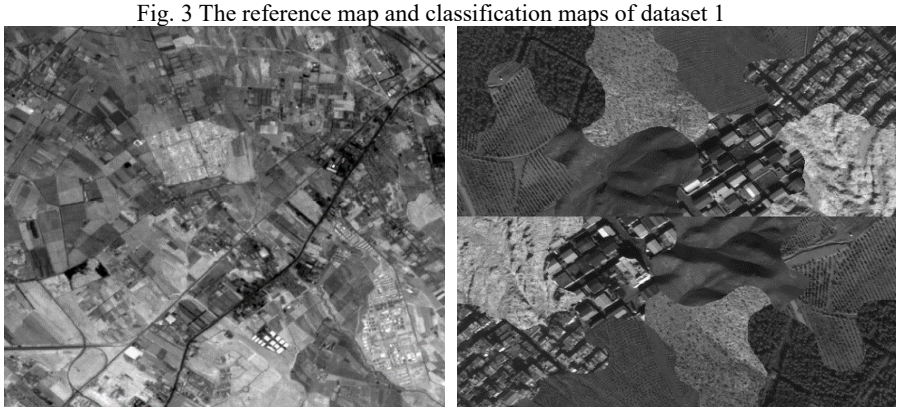

Fig.4. Panchromatic Images of Dataset 2 and Dataset 3

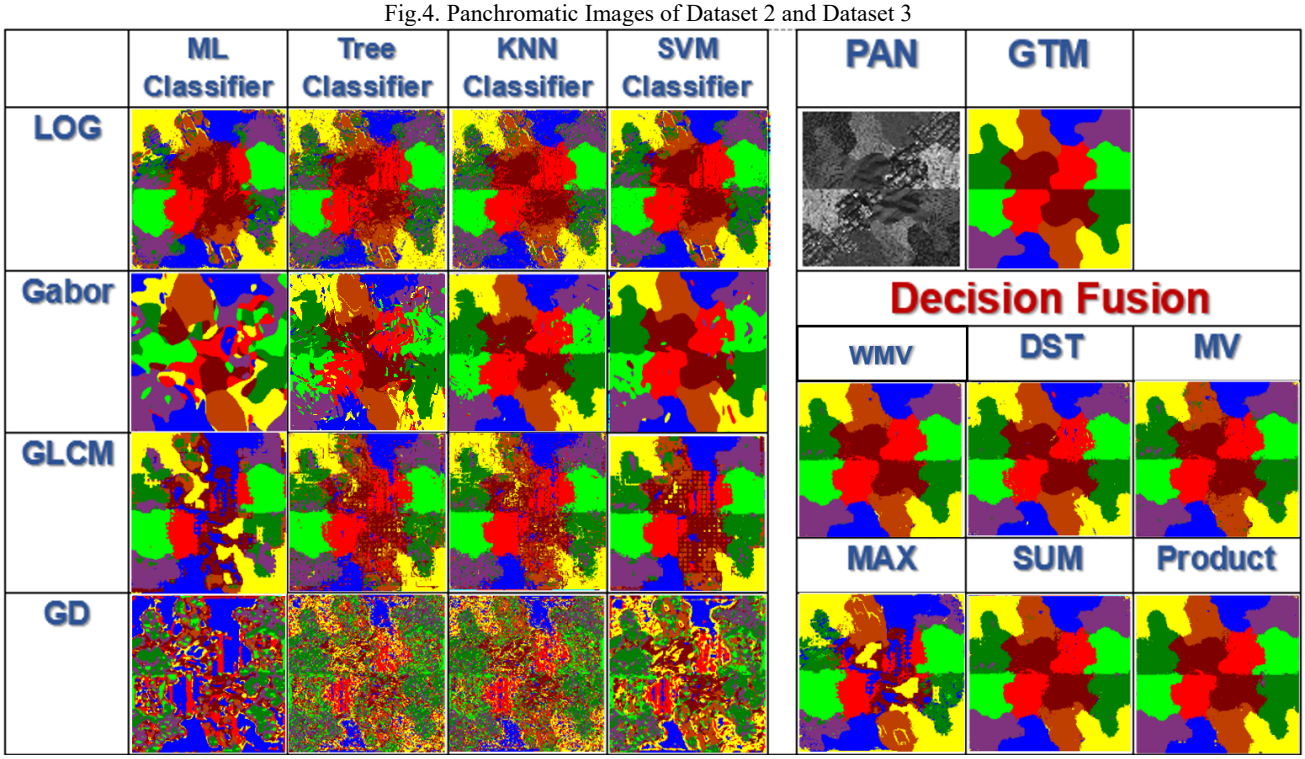

Fig. 5. The reference map and classification maps of Dataset 2

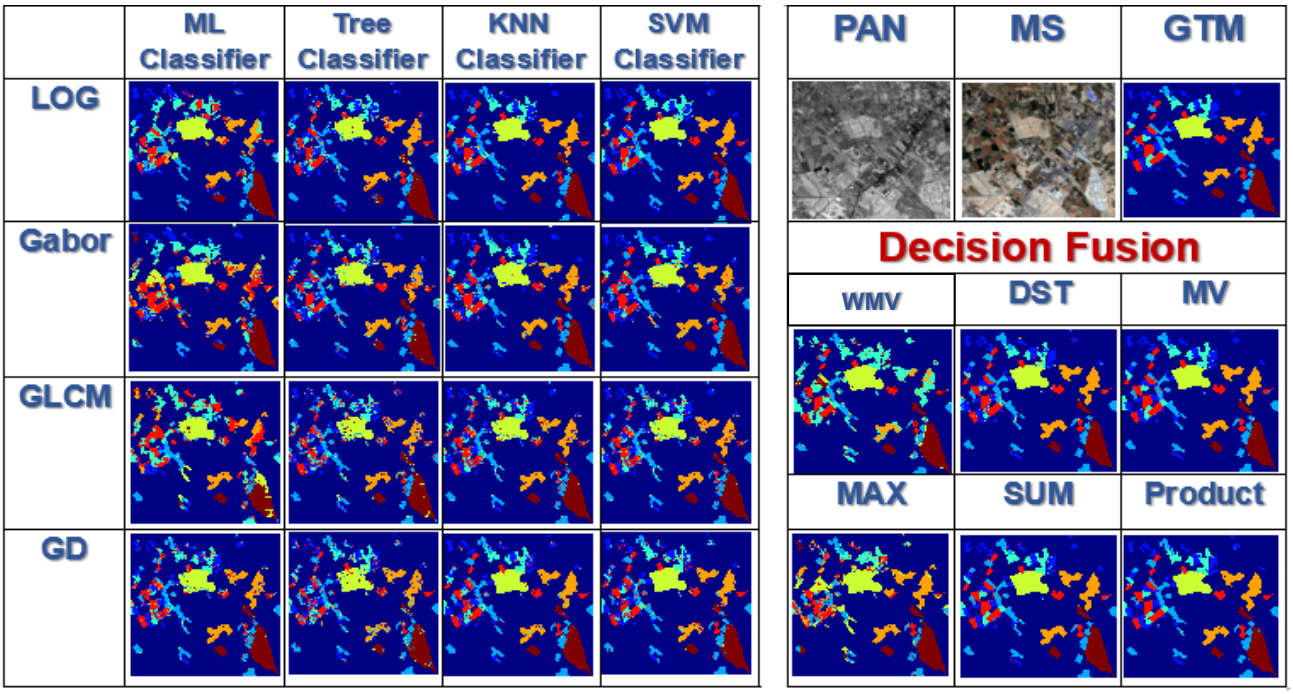

Fig. 6. The reference map and classification maps of Dataset3

Table III. Results of three dataset (first in red ,second in blue, third in green)

Decision Rule	Features	First dataset				Second dataset				Third dataset			
		AA	*OA*	*AV*	*K*	*AA*	*OA*	*AV*	*K*	*AA*	*OA*	*AV*	*K*
ML Classifier	LOG	25	28	27	22	73	73	73	71	66	65	66	59
	Gabor	59	52	48	47	57	56	57	52	58	57	60	51
	GLCM	70	71	62	66	65	65	67	62	54	53	55	46
	GD	34	22	20	16	36	35	36	30	27	24	27	13
Tree Classifier	LOG	34	47	35	39	71	71	71	68	66	66	65	60
	Gabor	76	84	78	81	82	82	82	80	77	77	76	73
	GLCM	73	80	73	77	72	72	73	70	60	61	60	54
	GD	27	42	28	32	39	39	39	34	28	28	27	15
KNN Classifier	LOG	43	53	44	46	82	82	82	80	82	81	80	78
	Gabor	89	90	89	88	91	91	92	90	90	91	89	89
	GLCM	82	87	83	85	78	79	79	77	72	72	72	67
	GD	33	46	34	37	48	48	49	44	39	37	35	25
SVM Classifier	LOG	38	56	47	47	78	78	78	76	81	81	81	78
	Gabor	76	83	85	80	92	92	92	91	90	91	91	89
	GLCM	79	85	83	83	76	76	76	74	71	72	71	67
	GD	27	52	43	42	45	45	45	40	40	40	40	37
Decision fusion	WMV	90	93	96	89	96	96	96	95	93	93	93	92
	DST	91	93	96	90	95	95	95	95	93	94	93	92
	MV	87	92	95	86	93	94	95	93	91	91	91	90
	Max	81	80	76	78	85	74	66	72	70	73	76	68
	Product	85	86	85	84	96	96	97	96	77	78	89	72
	Sum	85	87	83	84	95	96	96	95	77	78	89	73

REFERENCES

[1] Maryam Imani and Hassan Ghassemian, "An overview on Spectral and Spatial Information Fusion for Hyperspectral Image Classification: Current Trends and Challenges, " vol. 59, pp. 59-83, Nov. 2020.

[2] H. Ghassemian, "A review of remote sensing image fusion methods," *Information Fusion,* vol. 32, no. 1 pp. 75-89, 2016.

[3] Lu, Dengsheng, and Qihao Weng. "A survey of image classification methods and techniques for improving classification performance." International journal of Remote sensing 28.5, pp.823-870, 2007.

[4] Beirami, Behnam Asghari, and Mehdi Mokhtarzade. "Spatial-spectral classification of hyperspectral images based on multiple fractal-based features." *Geocarto International* , 1-15 ,2020 .

[5] C. Liu, J. Li, L. He, A. Plaza, S. Li and B. Li, "Naive Gabor Networks for Hyperspectral Image N Classification," *IEEE Transactions on Neural Networks and Learning Systems, 2020.*

[6] M. Imani and H. Ghassemian, "Morphology-based structure-preserving projection for spectral–spatial feature extraction and classification of hyperspectral data," IET Image Processing, vol. 13, no. 2, pp. 270-279, Feb. 2019.

[7] A. Zehtabian and H. Ghassemian, "An Adaptive Pixon Extraction Technique for Multispectral/Hyperspectral Image Classification" IEEE Geoscience and Remote Sensing Letters, vol. 12, no. 4, April 2015.

[8] X. Jiang, Y. Zhang, Y. Li, S. Li, and Y.Zhang, "Hyperspectral image classification with transfer learning and Markov random fields," IEEE Geosci. Remote Sens. Lett., vol. 17, no. 3, pp. 544–548, Mar. 2020.

[9] S. Jia, Z. Lin, B. Deng, J. Zhu, and Q. Li, "Cascade superpixel regularized gabor feature fusion for hyperspectral image classification," IEEE Trans. Neural Netw. Learn. Syst., vol. 31, no. 5, pp. 1638–1652, May 2020.

[10] P. Duan, X. Kang, S. Li, P. Ghamisi, and J. A. Benediktsson, "Fusion of multiple edge-preserving operations for hyperspectral image classification," IEEE Trans. Geosci. Remote Sens., vol. 57, no. 12, pp. 10336–10349, Dec. 2019.

[11] S. Yang, J. Hou, Y. Jia, S. Mei, and Q. Du, "Hyperspectral image classification via sparse representation with incremental dictionaries," IEEE Geosci. Remote Sens. Lett., to be published, doi: 10.1109/LGRS.2019.

[12] F. Luo, L. Zhang, B. Du, and L. Zhang, "Dimensionality reduction with enhanced hybrid-graph discriminant learning for hyperspectral image classification," IEEE Trans. Geosci. Remote Sens., to be published, doi: 10.1109/TGRS.2020.

[13] F. Luo, L. Zhang, X. Zhou, T. Guo, Y. Cheng, and T. Yin, "Sparse-adaptive hypergraph discriminant analysis for hyperspectral image classification," IEEE Geosci. Remote Sens. Lett., vol. 17, no. 6, pp. 1082–1086, Jun. 2020.

[14] D. Hong, X. Wu, P. Ghamisi, J. Chanussot, N. Yokoya, and X. X. Zhu, "Invariant attribute profiles: A spatial-frequency joint feature extractor for hyperspectral image classification," IEEE Trans. Geosci. Remote Sens., vol. 58, no. 6, pp. 3791–3808, Jun. 2020.

[15] P. Ghamisi, R. Souza, J. A. Benediktsson, X. X. Zhu, L. Rittner, and R. A. Lotufo, "Extinction profiles for the classification of remote sensing data," IEEE Trans. Geosci. Remote Sens., vol. 54, no. 10, pp. 5631–5645, Oct. 2016.

[16] X. X. Zhu et al., "Deep learning in remote sensing: A comprehensive review and list of resources," IEEE Geosci. Remote Sens. Mag., vol. 5, no. 4, pp. 8–36, Dec. 2017.

[17] Fardin Mirzapour, Hassan Ghassemian, Fast GLCM and Gabor Filters for Texture Classification of Very High Resolution Remote Sensing Images, International Journal of Information & Communication Technology Research, vol. 7, No. 3,pp. 21-30, 2015.

[18] Kong, Hui, Hatice Cinar Akakin, and Sanjay E. Sarma. "A generalized Laplacian of Gaussian filter for blob detection and its applications." IEEE transactions on cybernetics 43.6 ,pp.1719-1733, 2013.

[19] Mirzapour, Fardin, and Hassan Ghassemian. "Multiscale gaussian derivative functions for hyperspectral image feature extraction." IEEE Geoscience and Remote Sensing Letters 13.4, pp. 525-529, 2016.

[20] FatihaBelmahdi, MouradLazri, FethiOuallouche, KarimLabadi, RafikAbsi, SoltaneAmeur, "Application of Dempster-Shafer theory for optimization of precipitation classification and estimation results from remote sensing data using machine learning". Remote Sensing Applications: Society and Environment. 2023, Vol 29, Article 100899.

[21] Ashkan Taghipour and Hassan Ghassemian, "Visual attention-driven framework to incorporate spatial-spectral features for hyperspectral anomaly detection", International Journal of Remote Sensing, vol. 42, no. 19, pp. 7454-7488, 2021.

[22] Rashidi, Ali, and Hassan Ghassemian. "Extended Dempster–Shafer theory for multi-system/sensor decision fusion." Commission IV Joint Workshop on Challenges in Geospatial Analysis, Integration and Visualization II. 2003.

[23] Ali J. Rashidi, M. Hassan Ghassemian, "A New Approach for Multi-System/Sensor Decision Fusion Based on Joint Measures" I. J. Information Acquisition 1(2): 109-120, 2004 .

[24] A. Rashidi and H. Ghassemian, "A New High Reliability and Dual Measure Method for Multi-System/Sensor Remote-Sensing Decision Fusion," Proceeding of ISPRS-2004, vol.3, pp. 541-546, July 2004.

[25] L. Dai, G. Zhang and R. Zhang, "RADANet: Road Augmented Deformable Attention Network for Road Extraction from Complex High-Resolution Remote-Sensing Images," in IEEE Trans. Geosci. Remote Sens., doi: 10.1109/TGRS.2023.3237561, Jun 2023.

[26] M. Stoimchev, D. Kocev, and S. Džeroski, "Deep Network Architectures as Feature Extractors for Multi-Label Classification of Remote Sensing Images," Remote Sensing, vol. 15, no. 2, p. 538, Jan. 2023, doi: 10.3390/rs15020538.